Model Predictive Control of Transitional Maneuvers for Adaptive Cruise Control Vehicles

Vibhor L. Bageshwar, William L. Garrard, and Rajesh Rajamani, *Member, IEEE*

***Abstract*—In this paper, model predictive control (MPC) is used to compute the spacing-control laws for transitional maneuvers (TMs) of vehicles equipped with adaptive cruise control (ACC) systems. A TM is required, for example, to establish a steady-state following distance behind a newly encountered vehicle traveling with a slower velocity. These spacing-control laws are computed by formulating the objective of a TM as an optimal control problem (OCP). The steady-state following distance, collision avoidance, and acceleration limits of the ACC vehicle are incorporated into the OCP as constraints. The spacing-control laws are then obtained by solving this constrained OCP by using a receding-horizon approach, where the acceleration command computed at each sampling instant is a function of the current measurements of range and range rate. A baseline scenario requiring a TM is used to evaluate and compare the performance of the MPC algorithm and the standard constant time gap (CTG) algorithm. The simulation results show that the ACC vehicle is able to perform the TM of the baseline scenario using the MPC spacing-control laws, whereas the ACC vehicle is unable to perform this TM using the CTG spacing-control laws. The success of the MPC spacing-control laws is shown to depend on whether collision avoidance and the acceleration limits of the ACC vehicle are explicitly incorporated into the formulation of the control algorithm.**

***Index Terms*—Adaptive cruise control (ACC), longitudinal vehicle control, model predictive control (MPC), transitional maneuvers (TMs).**

I. Introduction

ADAPTIVE cruise control (ACC) systems are extensions of standard cruise control (SCC) systems [1]. Whereas an SCC system provides a vehicle with one mode of longitudinal control (speed control), an ACC system provides a vehicle with two modes of longitudinal control (speed control and headway control). Headway control refers to the procedure through which a vehicle first establishes and then maintains a specified distance between itself and the immediately preceding vehicle [2]. A vehicle equipped with an ACC system (an ACC vehicle) uses an onboard radar that measures the range and range rate between itself and the preceding vehicle to enable headway control.

An ACC system uses its two modes of longitudinal control as follows. If there is no preceding vehicle, then the ACC system enables its speed-control mode and regulates the vehicle speed at a driver-defined setting. However, if the ACC vehicle is traveling using its speed-control mode and encounters a new, or target, vehicle traveling with a slower speed, then the ACC system must enable its headway-control mode to avoid a collision with the target vehicle.

Headway control consists of two phases of operation [2]: transitional and steady state. The procedure through which the ACC vehicle establishes the specified intervehicle distance (SIVD) behind the target vehicle is referred to as transitional operation and has two requirements. First, the ACC system must determine when to switch from its speed-control mode to its headway-control mode. Second, the ACC system must implement a control algorithm to maneuver the vehicle to the SIVD. This maneuver will be referred to as a transitional maneuver (TM). The procedure through which the ACC vehicle maintains the SIVD is referred to as steady-state operation.

A. Steady-State Operation

Steady-state operation [3] has been a subject of intense study and has two requirements. First, the steady-state spacing policy and the corresponding SIVD must be selected. Second, the ACC system must implement a control algorithm that maintains the SIVD regardless of the maneuver performed by the target vehicle. This control algorithm must also provide the ACC vehicle with individual vehicle stability and string stability, if applicable. The following three general steady-state spacing policies have been defined [4]: the constant distance spacing policy, the constant time gap (CTG) spacing policy, and the constant safety factor spacing policy. The success of these spacing policies has been shown to depend on the real-time information the ACC system has available regarding both the target vehicle and, if applicable, other vehicles preceding the target vehicle [5]. For an autonomous system, such as an ACC system, a CTG spacing policy and the associated CTG control algorithm have been shown to satisfy the requirements of steady-state operation.

B. Transitional Operation

A previous study of the transitional operation problem for ACC vehicles [2] made use of the kinematic relationships between range and range rate to illustrate the requirements of transitional operation. These kinematic relationships can be used to construct a range versus range rate diagram, as shown in Fig. 1. In Fig. 1, range refers to the relative distance between the target vehicle and the ACC vehicle and, thus, a negative range indicates that the ACC vehicle has collided with the target vehicle. Range rate refers to the relative speed between the target vehicle

Manuscript received December 16, 2003; revised April 12, 2004 and May 21, 2004. This work was supported by NASA under Grant NGT5-40086 and by the Intelligent Transportation System (ITS) Institute, University of Minnesota, Minneapolis.

V. L. Bageshwar and W. L. Garrard are with the Department of Aerospace Engineering and Mechanics, University of Minnesota, Minneapolis, MN 55455 USA (e-mail: vbageshw@aem.umn.edu).

R. Rajamani is with the Department of Mechanical Engineering, University of Minnesota, Minneapolis, MN 55455 USA.

Digital Object Identifier 10.1109/TVT.2004.833625

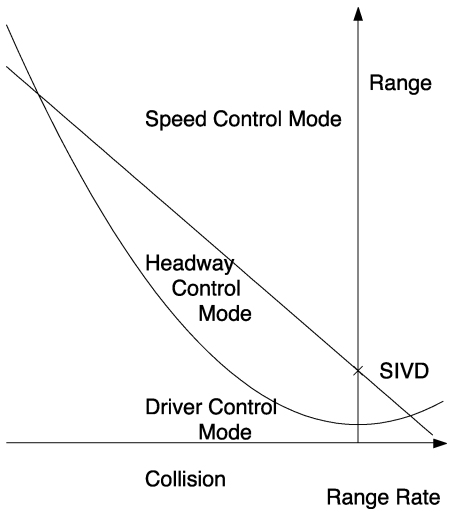

Fig. 1. Range versus range rate diagram.

and the ACC vehicle and, thus, a negative range rate indicates that the ACC vehicle is faster than the target vehicle.

This figure is divided into three regions, where each region corresponds to a transitional control mode of the ACC vehicle. The solid lines represent both the boundaries of these regions and the switching conditions between these regions. The ACC system can then compare measurements of range and range rate to the diagram to select the control mode and to determine when to switch between these modes. The third region of this diagram refers to the driver-control mode. This region is included in the diagram because there exist scenarios for which the measurements of range and range rate will indicate that a maximum deceleration by the ACC vehicle is unable to prevent a collision with the target vehicle. For these scenarios, the driver of the ACC vehicle must intervene and perform an alternative maneuver, such as a lane change, to prevent a collision with the target vehicle.

The kinematic relationships between range and range rate can be used to formulate an algorithm to perform the TM and to establish the SIVD. The premise of the algorithm is for the ACC vehicle to establish the SIVD by tracking a trajectory that corresponds to the switching line between the speed-control and headway-control modes. Any vehicle trajectory that tracks this switching line will have a linear relationship between range and range rate. The actual implementation of this algorithm depends on the encounter scenario, because it is unlikely that the measurements of range and range rate are on the linear switching line.

The transitional operation problem has also been studied for platoons of vehicles in automated highway systems (AHS) [6]–[9]. For AHS, transitional operation refers to the merging of two platoons to form a single platoon. In general, ACC vehicles use the CTG spacing policy, whereas AHS platoons use the constance distance spacing policy, where the SIVD is on the order of a few meters. As a result, these AHS studies formulated algorithms to perform the TM and to establish the SIVD by using the following two step procedure. First, trajectories were designed to perform the TM that minimized the overshoot of the SIVD. Second, control algorithms were implemented to obtain spacing-control laws that track these trajectories.

In [6], an open-loop trajectory was designed to perform the TM, assuming that the nonmerging platoon maintained a constant velocity during the execution of the TM. In [7] and [8], a closed-loop trajectory was designed to perform the TM, assuming that the nonmerging platoon could accelerate or decelerate during the execution of the TM. This trajectory was based on the merging platoon maintaining a safe velocity throughout the TM. A safe velocity refers to a constraint on the range rate that ensures that the two platoons do not collide at a high relative velocity. In [9], a sliding surface controller was used to compute the spacing-control laws that track the closed-loop trajectory designed in [7] and [8].

C. Objectives and Methodology of the Current Work

The objectives of this paper are to use model predictive control (MPC) to design the spacing-control laws for TMs of an ACC vehicle and, then, to evaluate the performance of these MPC spacing-control laws. MPC is based on solving an online OCP by using a receding-horizon approach to obtain state feedback control laws [10]–[12]. A TM is defined as a maneuver performed by the ACC vehicle to establish the SIVD using measurements of range, range rate, and the ACC vehicle velocity and acceleration with the following requirements placed on the maneuver. First, the ACC vehicle must establish a zero-range rate at the SIVD. Second, the ACC vehicle must avoid a collision with the target vehicle while performing the TM.

The MPC spacing-control laws for the TM problem are computed by formulating a finite-time constrained OCP (FTCOCP) with a discrete-time quadratic performance index. The ACC vehicle is modeled as a linear dynamical system with nonsymmetric acceleration limits. The objective and requirements of the TM problem are incorporated into the FTCOCP through the problem constraints. The objective of establishing the SIVD with a zero-range rate is formulated as a terminal constraint. The requirement of collision avoidance is formulated as a state constraint. Furthermore, the MPC spacing-control laws must also satisfy the physical constraints of the ACC vehicle. Therefore, the acceleration limits of the ACC vehicle are incorporated into the FTCOCP as control constraints. The solution to this FTCOCP is computed by reformulating the FTCOCP as a mathematical program (MP) [13].

The FTCOCP can be reformulated as an MP by rewriting the state vector of the discrete-time ACC vehicle model as a function of its initial conditions and the control sequence throughout the entire time horizon of the FTCOCP. This version of the state vector is then substituted into the performance index and the constraint equations of the FTCOCP to form the MP. The solution of the resulting MP is then obtained by using a mathematical programming solver and yields an open-loop control sequence throughout the entire time horizon of the FTCOCP.

The state feedback spacing-control law used to perform the TM is then computed using a receding-horizon approach. At regular sampling times, the ACC system measures the range, range rate, and ACC vehicle velocity and acceleration. Using these measurements, the spacing error, range rate, and ACC vehicle acceleration can be combined to form an error vector. The

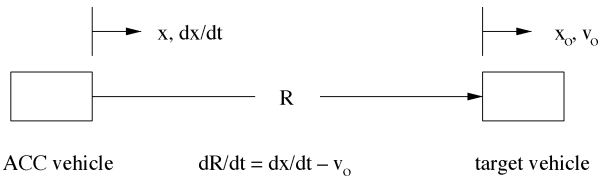

Fig. 2. Definition of the two-vehicle system.

spacing error refers to the difference between the SIVD and measured range. Using this error vector as the initial condition, the MP is formed and solved to obtain an open-loop control sequence throughout the time horizon of the FTCOCP. However, only the first control action of the open-loop sequence is applied to the ACC vehicle. If these measurements and the subsequent computation of the open-loop control sequence were made at each sampling time during the execution of the TM, then a state feedback spacing-control law is obtained, because the control action applied at each sampling time depends on the current error vector.

The advantage of using the MPC algorithm for the TM problem is that the same problem formulation can be used to compute the spacing-control laws for all feasible initial conditions of an encounter scenario with the target vehicle, regardless of the maneuver performed by the target vehicle. Furthermore, the objective of establishing the SIVD with zero-range rate, collision avoidance, and the acceleration limits of the ACC vehicle can be incorporated into the FTCOCP and the resulting MP as constraints. Therefore, the solution of the MP formulated at each sampling time during the execution of the TM must satisfy these constraints throughout the time horizon of the FTCOCP. It should be noted that the MPC spacing-control laws are not designed to track trajectories that maneuver the ACC vehicle to the SIVD. The disadvantage of the MPC algorithm is that the computation time required to solve an online MP could exceed the sampling time of the ACC system.

This paper is organized as follows. In Section II, the control architecture of an ACC vehicle is described and the ACC vehicle model used to compute the spacing-control laws is defined. In Section III, the synthesis of the MPC algorithm is described including the formulation of the FTCOCP and its reformulation as an MP. In Section IV, a baseline scenario requiring a TM is defined. For this scenario, the simulated response of the ACC vehicle to the MPC spacing-control laws and the spacing-control laws computed using the standard CTG control algorithm are evaluated and compared. In Section V, the conclusion is drawn.

II. ACC Vehicle Model

A two-vehicle system consisting of the ACC vehicle and the target vehicle will be used to compute the spacing-control laws for TMs of the ACC vehicle. The onboard radar of the ACC vehicle will be assumed capable of measuring the range R and the range rate $\dot{\mathrm{R}}$ (Fig. 2). The definition of range will remain as defined in Section I. However, the definition of range rate will be modified to refer to the relative speed between the ACC vehicle and the target vehicle. This definition of range rate will be used throughout the remaining sections of this paper. It will be assumed that the onboard radar is capable of measuring a maximum range of 110 m. In addition to the measurements of range and range rate, only the measurements of the ACC vehicle velocity and acceleration will be used to compute the spacing-control laws.

The longitudinal control system of an ACC vehicle is commonly modeled using a two-level control architecture consisting of upper- and lower-level controllers [1]. The upper-level controller uses the four available measurements outlined above to compute a spacing-control law or a sequence of acceleration commands to perform the maneuver required of the ACC vehicle. The lower-level controller uses throttle and braking commands to track the spacing-control law computed by the upper-level controller. However, the lower-level controller has a finite bandwidth and, thus, the ACC vehicle will be unable to track the acceleration commands instantaneously. Therefore, the ACC vehicle model must reflect the finite bandwidth of the lower-level controller.

The ACC vehicle model used to design the spacing-control laws will be a first-order model where the acceleration commands sent to the lower-level controller are considered to be the control input [1]. The following variables will be used to refer to the states of the two vehicle system, as shown in Fig. 2. x_o and v_o refer to the absolute position and velocity of the target vehicle, respectively. x, $\dot{x}$, and $\ddot{x}$ refer to the absolute position, velocity, and acceleration of the ACC vehicle, respectively. u refers to the acceleration commands computed by the upper-level controller. The ACC vehicle model can then be defined as

$$\tau \frac{d}{dt}\ddot{x}(t) + \ddot{x}(t) = u(t) \tag{1}$$

$$\dot{x}(t) \geq 0 \tag{2}$$

$$u_{\min} \leq u(t) \leq u_{\max} \tag{3}$$

where τ refers to the time lag corresponding to the finite bandwidth of the lower-level controller. Two physical constraints of the ACC vehicle have been included in this model as well. First, the vehicle will not be permitted to have a negative velocity during the TM [see (2)] and, second, the vehicle is assumed to have nonsymmetric acceleration limits [see (3)]. For control design and simulation purposes, τ will be assumed equal to 0.5 s, $u_{\max}$ will be assumed equal to 0.25 g, and $u_{\min}$ will be assumed equal to -0.5 g.

A continuous-time state-space representation of the ACC vehicle model can be written as

$$\frac{d}{dt}\begin{pmatrix} x(t) \\ \dot{x}(t) \\ \ddot{x}(t) \end{pmatrix} = \begin{pmatrix} 0 & 1 & 0 \\ 0 & 0 & 1 \\ 0 & 0 & -\frac{1}{\tau} \end{pmatrix}\begin{pmatrix} x(t) \\ \dot{x}(t) \\ \ddot{x}(t) \end{pmatrix} + \begin{pmatrix} 0 \\ 0 \\ \frac{1}{\tau} \end{pmatrix} u(t). \tag{4}$$

An equivalent discrete-time state-space representation of the ACC vehicle model can be obtained by using the following forward difference approximations [12]:

$$\dot{x}(t) = \frac{x(t+T) - x(t)}{T} \tag{5}$$

$$\ddot{x}(t) = \frac{\dot{x}(t+T) - \dot{x}(t)}{T} \tag{6}$$

$$\frac{d}{dt}\ddot{x}(t) = \frac{\ddot{x}(t+T) - \ddot{x}(t)}{T} \tag{7}$$

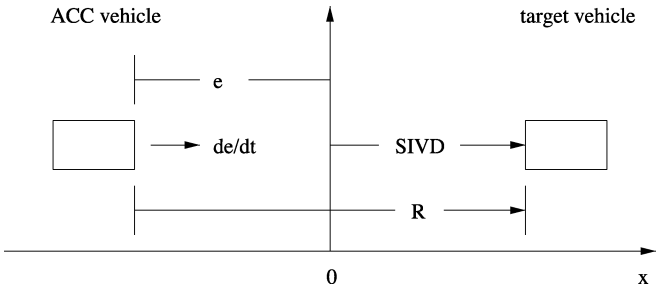

Fig. 3. Coordinate frame for TMs.

where T refers to the sampling time of the ACC system. If (7) is substituted into (1), then (1), (5), and (6) can be rewritten as

$$\begin{pmatrix} x(t+T) \\ \dot{x}(t+T) \\ \ddot{x}(t+T) \end{pmatrix} = \begin{pmatrix} 1 & T & 0 \\ 0 & 1 & T \\ 0 & 0 & 1-\frac{T}{\tau} \end{pmatrix} \begin{pmatrix} x(t) \\ \dot{x}(t) \\ \ddot{x}(t) \end{pmatrix} + \begin{pmatrix} 0 \\ 0 \\ \frac{T}{\tau} \end{pmatrix} u(t). \tag{8}$$

The continuous-time ACC vehicle model will be used to define feasible initial conditions for the TM problem. The discrete-time ACC vehicle model will be used to design the MPC spacing-control laws for the TM problem.

III. Synthesis of the MPC Algorithm

This section describes the synthesis of the MPC algorithm used to compute the spacing-control laws for the TM problem. First, a coordinate frame is defined to simplify the TM problem. Second, feasible initial conditions of the two-vehicle system are defined, for which the ACC vehicle can establish the SIVD. Third, the underlying FTCOCP of the TM problem is formulated. Fourth, the FTCOCP is reformulated as an MP. Fifth, the receding-horizon approach is explained in further detail to show how a state feedback spacing-control law is obtained.

A. Coordinate Frame for TMs

In this section, a coordinate frame will be defined in which the state variables of the ACC vehicle are defined relative to the SIVD (Fig. 3). The frame travels with a velocity equal to that of the target vehicle and the origin of this frame is located at the SIVD. Therefore, the objective of the TM problem can be restated as to maneuver the ACC vehicle to the origin of this frame such that there is a zero-range rate once the vehicle establishes the origin.

Using this frame, the discrete-time ACC vehicle model can be rewritten as

$$\mathbf{e}_{k+1} = \Phi \mathbf{e}_k + \Gamma \mathbf{u}_k \tag{9}$$

$$\mathbf{y}_k = \Lambda \mathbf{e}_k \tag{10}$$

where Φ and Γ are defined in (8). $\mathbf{e}_k$ and Λ are defined as

$$\mathbf{e}_k = \begin{pmatrix} e_k \\ \dot{e}_k \\ \ddot{e}_k \end{pmatrix} = \begin{pmatrix} -(\mathrm{R}-\mathrm{SIVD}) \\ \dot{\mathrm{R}} \\ \ddot{x}_k \end{pmatrix}$$

$$\Lambda = \begin{pmatrix} 1 & 0 & 0 \\ 0 & -1 & 0 \end{pmatrix}. \tag{11}$$

In (11), e_k refers to the spacing error, $\dot{e}_k$ refers to the range rate, $\ddot{e}_k$ refers to the absolute acceleration of the ACC vehicle, and $\mathbf{e}_k$ will be referred to as the error vector. This vector has been selected to reflect the quantities measured by the ACC system. The SIVD depends on the selection of the spacing policy and can be computed using the quantities measured by the ACC system. This coordinate frame will be referred to as the TM frame and used throughout the remaining sections of this paper.

Since the TM frame is traveling with a velocity equal to that of the target vehicle, the position of the target vehicle in the frame can change during the TM. If the target vehicle travels with a constant velocity, then the position of the target vehicle is fixed with respect to the origin of the frame. However, if the target vehicle accelerates or decelerates between sampling times during the TM, then the velocity of the TM frame will change accordingly at the next sampling time to reflect the measurement update. Furthermore, if the CTG spacing policy is adopted by the ACC vehicle, then both the SIVD and the position of the target vehicle in the TM frame will change accordingly at the next sampling time as well.

B. Feasible Initial Conditions

The initial conditions of the TM problem describe the measurements of the range, range rate, and the ACC vehicle velocity and acceleration when the target vehicle is first encountered. An encounter scenario will be considered feasible if the ACC vehicle can decelerate from its initial measured velocity to the velocity of the target vehicle while avoiding a collision with the target vehicle. The minimum range required for the ACC vehicle to decelerate to the velocity of the target vehicle can be obtained by computing the range required to perform the maneuver using the maximum available deceleration. It will be assumed that the target vehicle travels with a constant velocity throughout this maximum deceleration maneuver and that the ACC vehicle is traveling using its speed-control mode when it encounters the target vehicle.

The continuous-time ACC vehicle model can be written as

$$\dot{\mathbf{x}}(t) = \mathbf{A}\mathbf{x}(t) + \mathbf{B}\mathbf{u}(t) \tag{12}$$

where $\mathbf{A}$ and $\mathbf{B}$ have been defined in (4) and where $\mathbf{x}(t)$ is defined as

$$\mathbf{x}(t) = \begin{pmatrix} x(t) \\ \dot{\mathrm{R}}(t) \\ \ddot{x}(t) \end{pmatrix}. \tag{13}$$

The solution to (12) can be written as [14]

$$\mathbf{x}(t) = e^{\mathbf{A}t}\mathbf{x}(0) + \int_0^t e^{\mathbf{A}(t-\eta)}\mathbf{B}\mathbf{u}(\eta)d\eta \tag{14}$$

where the initial and final times of the maximum deceleration maneuver have been set equal to 0 and t, respectively. $e^{\mathbf{A}t}$ can

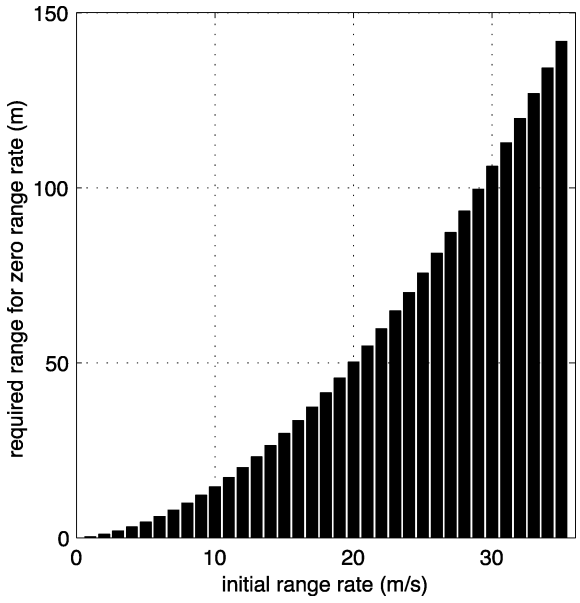

Fig. 4. Feasible initial conditions for TMs.

be determined by computing the inverse Laplace transform of $(s\mathbf{I}-\mathbf{A})^{-1}$ [14]

$$s\mathbf{I}-\mathbf{A}=\begin{pmatrix} s & -1 & 0 \\ 0 & s & -1 \\ 0 & 0 & s+2 \end{pmatrix}$$

$$(s\mathbf{I}-\mathbf{A})^{-1}=\frac{1}{s^2(s+2)}\begin{pmatrix} s(s+2) & s+2 & 1 \\ 0 & s(s+2) & s \\ 0 & 0 & s^2 \end{pmatrix}$$

and thus

$$e^{\mathbf{A}t}=\begin{pmatrix} 1 & t & -\frac{1}{4}+\frac{t}{2}+\frac{e^{-2t}}{4} \\ 0 & 1 & \frac{1}{2}-\frac{e^{-2t}}{2} \\ 0 & 0 & e^{-2t} \end{pmatrix}. \tag{15}$$

Since both vehicles are initially assumed to be traveling with constant velocity, the initial conditions of the maximum deceleration maneuver $\mathbf{x}(0)$ depend only on the initial measurement of range rate and can be written as

$$\mathbf{x}(0)=\begin{pmatrix} 0 \\ \dot{x}(0)-v_0 \\ 0 \end{pmatrix}. \tag{16}$$

Given $e^{\mathbf{A}t}$ and $\mathbf{x}(0)$ for the maximum deceleration maneuver, (13) can be written as

$$x(t)=(\dot{x}(0)-v_0)\,t+\left(\frac{1}{4}-\frac{t}{2}+\frac{t^2}{2}-\frac{1}{4}e^{-2t}\right)u_{\min} \tag{17a}$$

$$\dot{\mathrm{R}}(t)=\dot{x}(0)-v_0+\left(-\frac{1}{2}+t+\frac{1}{2}e^{-2t}\right)u_{\min} \tag{17b}$$

$$\ddot{x}(t)=(1-e^{-2t})u_{\min}. \tag{17c}$$

Fig. 4 shows the minimum range required for the ACC vehicle to perform the maximum deceleration maneuver for various initial range rates. Fig. 4 has the following interpretation. If the ACC vehicle encounters the target vehicle with an initial measured range rate of 20 m/s, then the ACC vehicle will require an initial range of 50 m to perform a TM and avoid a collision with the target vehicle. Therefore, if the initial range is 60 m, then this encounter scenario is considered to be feasible. However, if the initial range is 40 m, then the ACC vehicle would be unable to perform a TM and avoid a collision with the target vehicle. Therefore, this encounter scenario is considered to be infeasible.

C. Formulation of the OCP

The control objective of the TM problem is to compute the spacing-control laws that will maneuver the ACC vehicle to the SIVD. This control objective and the other requirements of the TM problem can be formulated as an FTCOCP as follows. Given the initial error vector $\mathbf{e}(0)$, determine the control sequence $(\mathbf{u}_0,\ldots,\mathbf{u}_{N-1})$ that minimizes the performance index

$$\mathrm{J}=\mathbf{e}_N^T\mathbf{S}\mathbf{e}_N+\sum_{k=0}^{N-1}\left\{\mathbf{e}_k^T\mathbf{Q}\mathbf{e}_k+\mathbf{u}_k^T\mathbf{R}\mathbf{u}_k\right\} \tag{18}$$

subject to

$$\mathbf{e}_{k+1}=\Phi\mathbf{e}_k+\Gamma\mathbf{u}_k \tag{19a}$$

$$\mathbf{e}(0)\equiv\text{measured} \tag{19b}$$

with state and control constraints

$$\mathbf{y}_k=\begin{pmatrix} e_k \\ -\dot{e}_k \end{pmatrix}\le\begin{pmatrix} \text{SIVD} \\ v_o \end{pmatrix}=\mathbf{S}_c \tag{20}$$

$$u_{\min}\le\mathbf{u}_k\le u_{\max} \tag{21}$$

and with terminal, or final state, constraint

$$\mathbf{e}_N=\psi=\begin{pmatrix} 0 \\ 0 \\ 0 \end{pmatrix} \tag{22}$$

where N refers to the time horizon of the FTCOCP.

The FTCOCP has been formulated with a linear quadratic performance index (18) and with the final state fixed (22). $\mathbf{Q}$, $\mathbf{R}$, and $\mathbf{S}$ are weighting matrices where $\mathbf{S}$ is a weighting matrix for the final state. These three matrices are selected to satisfy the conditions [15]

$$\mathbf{Q}=\mathbf{Q}^T\ge\mathbf{0} \tag{23}$$

$$\mathbf{R}=\mathbf{R}^T>\mathbf{0} \tag{24}$$

$$\mathbf{S}=\mathbf{S}^T\ge\mathbf{0}. \tag{25}$$

In this formulation, $\mathbf{e}_k$ refers to the predicted error vector throughout the time horizon N. $\mathbf{e}_k$ is obtained by applying the computed control sequence $(\mathbf{u}_0,\ldots,\mathbf{u}_{N-1})$ using the measured error vector $\mathbf{e}(0)$ as the initial condition.

The objectives and requirements of the TM problem have been explicitly incorporated into the FTCOCP using the error vector and TM frame. The objective of establishing the SIVD with a zero-range rate has been formulated as a final state constraint (22). $\mathbf{e}_N$ can be set equal to ψ through the definition of the TM frame. Collision avoidance has been formulated as a state constraint (20). Furthermore, the condition ensuring the ACC vehicle has a nonnegative velocity (2) has also been included as a state constraint. The acceleration limits of the ACC vehicle have been formulated as control constraints (21). These state

and control constraints are conditions that must be satisfied at every instant k of the time horizon N [12].

D. Formulation of the MP

One approach that can be used to solve a FTCOCP and compute the optimal control sequence is to reformulate the FTCOCP as an MP [13]. The resulting MP can then be solved using a mathematical programming solver. An MP refers to an optimization problem of the form [16]

$$\inf_{\mathbf{z}\in\mathbf{Z}} \mathrm{F}(\mathbf{z},\mathbf{p}) \tag{26a}$$

subject to

$$\mathbf{g}(\mathbf{z},\mathbf{p}) \le \mathbf{0} \tag{26b}$$

$$\mathbf{h}(\mathbf{z},\mathbf{p}) = \mathbf{0}. \tag{26c}$$

In (26), F refers to the scalar cost function, $\mathbf{g}$ is a vector of g inequality constraints, and $\mathbf{h}$ is a vector of h equality constraints. $\mathbf{z}$ is a vector of variables to be determined for a vector of parameters $\mathbf{p}$. For the TM problem, $\mathbf{p}$ will refer to the initial error vector $\mathbf{e}(0)$. $\mathbf{Z}$ refers to the feasible set of all $\mathbf{z}$ that satisfy the constraint equations of the MP. A solution of this MP will be considered optimal $\mathbf{z}^*$ if $\mathbf{z}^*$ satisfies the two following conditions. First, $\mathbf{z}^*$ must be feasible $\mathbf{z}^* \in \mathbf{Z}$. Second, $\mathbf{z}^*$ must satisfy the condition

$$\mathrm{F}(\mathbf{z}^*) \le \mathrm{F}(\mathbf{z}) \tag{27}$$

for any $\mathbf{z} \in \mathbf{Z}$.

A three-step procedure can be used to reformulate the FTCOCP as an MP [12]. First, the predicted error vector $\mathbf{e}_k$ is written as a function of the initial error vector $\mathbf{e}(0)$ and the control sequence $(\mathbf{u}_0,\ldots,\mathbf{u}_{k-1})$ as

$$\mathbf{e}_k = \Phi^k \mathbf{e}(0) + \sum_{l=0}^{k-1} \Phi^l \Gamma \mathbf{u}_{k-1-l} \tag{28}$$

where $k = 1,\ldots,N$. Equation (28) can also be written in matrix form as

$$\mathbf{E} = \bar{\mathbf{A}}\mathbf{e}(0) + \bar{\mathbf{B}}\mathbf{U} \tag{29}$$

where

$$\mathbf{E} = \begin{pmatrix} \mathbf{e}_1 \\ \vdots \\ \mathbf{e}_N \end{pmatrix}$$

$$\mathbf{U} = \begin{pmatrix} \mathbf{u}_0 \\ \vdots \\ \mathbf{u}_{N-1} \end{pmatrix}$$

$$\bar{\mathbf{A}} = \begin{pmatrix} \Phi \\ \vdots \\ \Phi^N \end{pmatrix}$$

$$\bar{\mathbf{B}} = \begin{pmatrix} \Gamma & \mathbf{0} & \ldots & \mathbf{0} \\ \Phi\Gamma & \Gamma & \ddots & \vdots \\ \vdots & \vdots & \ddots & \mathbf{0} \\ \Phi^{N-1}\Gamma & \Phi^{N-2}\Gamma & \ldots & \Gamma \end{pmatrix}.$$

Second, the performance index, state constraints, and control constraints are written in a matrix form similar to that of (29). Third, the expressions for $\mathbf{e}_k$ are then directly substituted into the performance index and the three constraint equations of the FTCOCP.

The performance index (18) can be written in matrix form as

$$\begin{aligned} \mathrm{J} &= \mathbf{e}_N^T\mathbf{S}\mathbf{e}_N + \mathbf{e}_0^T\mathbf{Q}\mathbf{e}_0 + \cdots + \mathbf{e}_{N-1}^T\mathbf{Q}\mathbf{e}_{N-1} + \mathbf{u}_0^T\mathbf{R}\mathbf{u}_0 \\ &\quad + \cdots + \mathbf{u}_{N-1}^T\mathbf{R}\mathbf{u}_{N-1} \\ &= \mathbf{e}_0^T\mathbf{Q}\mathbf{e}_0 + \mathbf{E}^T\bar{\mathbf{Q}}\mathbf{E} + \mathbf{U}^T\bar{\mathbf{R}}\mathbf{U} \end{aligned} \tag{30}$$

where

$$\bar{\mathbf{Q}} = \begin{pmatrix} \mathbf{Q} & \mathbf{0} & \ldots & \mathbf{0} \\ \mathbf{0} & \ddots & \ddots & \vdots \\ \vdots & \ddots & \mathbf{Q} & \mathbf{0} \\ \mathbf{0} & \ldots & \mathbf{0} & \mathbf{S} \end{pmatrix}$$

$$\bar{\mathbf{R}} = \begin{pmatrix} \mathbf{R} & \mathbf{0} & \ldots & \mathbf{0} \\ \mathbf{0} & \mathbf{R} & \ddots & \vdots \\ \vdots & \ddots & \ddots & \mathbf{0} \\ \mathbf{0} & \ldots & \mathbf{0} & \mathbf{R} \end{pmatrix}.$$

If (29) is substituted into (30), then the performance index can be rewritten as

$$\begin{aligned} \mathrm{J}\big(\mathbf{U},\mathbf{e}(0)\big) &= \mathbf{e}_0^T\mathbf{Q}\mathbf{e}_0 + \left\{\bar{\mathbf{A}}\mathbf{e}(0) + \bar{\mathbf{B}}\mathbf{U}\right\}^T \bar{\mathbf{Q}} \left\{\bar{\mathbf{A}}\mathbf{e}(0) + \bar{\mathbf{B}}\mathbf{U}\right\} \\ &= \mathbf{e}_0^T\{\mathbf{Q} + \bar{\mathbf{A}}^T\bar{\mathbf{Q}}\bar{\mathbf{A}}\}\mathbf{e}_0 + \mathbf{U}^T\mathbf{H}\mathbf{U} + 2\mathbf{G}\mathbf{U} \end{aligned} \tag{31}$$

where

$$\mathbf{H} = \bar{\mathbf{R}} + \bar{\mathbf{B}}^T\bar{\mathbf{Q}}\bar{\mathbf{B}}$$

$$\mathbf{G} = \mathbf{e}(0)^T\bar{\mathbf{A}}^T\bar{\mathbf{Q}}\bar{\mathbf{B}}.$$

If (28) is substituted into (22), then the final state constraint can be written as

$$\begin{aligned} \psi &= \Phi^N\mathbf{e}(0) + (\Phi^{N-1}\Gamma \quad \Phi^{N-2}\Gamma \quad \ldots \quad \Gamma)\mathbf{U} \\ \mathbf{L}_{EQ}\mathbf{U} &= \mathbf{M}_{EQ} \end{aligned} \tag{32}$$

where

$$\mathbf{L}_{EQ} = (\Phi^{N-1}\Gamma \quad \Phi^{N-2}\Gamma \quad \ldots \quad \Gamma)$$

$$\mathbf{M}_{EQ} = \psi - \Phi^N\mathbf{e}(0).$$

The state and control constraints (20) and (21) can be written in matrix form as

$$\bar{\mathbf{C}}\mathbf{E} \le \bar{\mathbf{S}}_c \tag{33}$$

where

$$\bar{\mathbf{C}} = \begin{pmatrix} \Lambda & \mathbf{0} & \ldots & \mathbf{0} \\ \mathbf{0} & \Lambda & \ddots & \vdots \\ \vdots & \ddots & \ddots & \mathbf{0} \\ \mathbf{0} & \ldots & \mathbf{0} & \Lambda \end{pmatrix}$$

$$\bar{\mathbf{S}}_c = \begin{pmatrix} \mathbf{S}_c \\ \vdots \\ \mathbf{S}_c \end{pmatrix}$$

and

$$\mathbf{U} \le \mathbf{U}_{\max} \tag{34a}$$

$$-\mathbf{U} \le -\mathbf{U}_{\min} \tag{34b}$$

where

$$\mathbf{U}_{\max} = \begin{pmatrix} u_{\max} \\ \vdots \\ u_{\max} \end{pmatrix}$$
$$\mathbf{U}_{\min} = \begin{pmatrix} u_{\min} \\ \vdots \\ u_{\min} \end{pmatrix}.$$

If (29) is substituted into (33), then the state constraints can be rewritten as

$$\begin{aligned} \bar{\mathbf{C}}\left(\bar{\mathbf{A}}\mathbf{e}(0) + \bar{\mathbf{B}}\mathbf{U}\right) &\leq \bar{\mathbf{S}}_c \\ \bar{\mathbf{C}}\bar{\mathbf{B}}\mathbf{U} &\leq \bar{\mathbf{S}}_c - \bar{\mathbf{C}}\bar{\mathbf{A}}\mathbf{e}(0). \end{aligned} \tag{35}$$

Equations (34) and (35) can be written in the compact notation

$$\mathbf{L}_{\text{IN}}\mathbf{U} \leq \mathbf{M}_{\text{IN}} \tag{36}$$

where

$$\mathbf{L}_{\text{IN}} = \begin{pmatrix} \bar{\mathbf{C}}\bar{\mathbf{B}} \\ \mathbf{I} \\ -\mathbf{I} \end{pmatrix}$$
$$\mathbf{M}_{\text{IN}} = \begin{pmatrix} \bar{\mathbf{S}}_c - \bar{\mathbf{C}}\bar{\mathbf{A}}\mathbf{e}(0) \\ \mathbf{U}_{\max} \\ -\mathbf{U}_{\min} \end{pmatrix}.$$

In summary, the FTCOCP can be written as the following MP:

$$\min_{\mathbf{U}} \mathbf{U}^T\mathbf{H}\mathbf{U} + 2\mathbf{G}\big(\mathbf{e}(0)\big)\mathbf{U} \tag{37a}$$

subject to

$$\mathbf{L}_{\text{IN}}\mathbf{U} \leq \mathbf{M}_{\text{IN}}\big(\mathbf{e}(0)\big) \tag{37b}$$
$$\mathbf{L}_{EQ}\mathbf{U} = \mathbf{M}_{EQ}\big(\mathbf{e}(0)\big). \tag{37c}$$

This MP has a quadratic cost function and is referred to as a quadratic program (QP) [16]. The $\mathbf{e}_0^T\{\mathbf{Q} + \bar{\mathbf{A}}^T\bar{\mathbf{Q}}\bar{\mathbf{A}}\}\mathbf{e}_0$ term of the performance index (31) is constant and is omitted from the cost function of the QP. The state and control constraints of the FTCOCP have been reformulated as the inequality constraints of the QP. The final state constraint of the FTCOCP has been reformulated as the equality constraints of the QP. The parameters of the QP are the initial error vector $\mathbf{e}(0)$ of the TM problem. The matrices $\mathbf{H}$, $\mathbf{L}_{\text{IN}}$, and $\mathbf{L}_{EQ}$ are fixed. The matrices $\mathbf{G}$, $\mathbf{M}_{\text{IN}}$, and $\mathbf{M}_{EQ}$ are functions of $\mathbf{e}(0)$ and become fixed once $\mathbf{e}(0)$ is measured. The solution of the QP yields an optimal open-loop control sequence $\mathbf{U}^{ol}$, where

$$\mathbf{U}^{ol} = \begin{pmatrix} \mathbf{u}_0^* \\ \vdots \\ \mathbf{u}_{N-1}^* \end{pmatrix} \tag{38}$$

throughout the time horizon of the FTCOCP.

It should be noted that if a QP is convex, then a local optimal solution of the QP is also a global optimal solution [16]. A QP is convex if its cost function and inequality constraints are convex and if its equality constraints are affine. A cost function of the form

$$\mathrm{F} = \mathbf{z}^T\mathbf{a}\mathbf{z} + 2\mathbf{b}^T\mathbf{z} + c \tag{39}$$

where $\mathbf{a} = \mathbf{a}^T$ is convex if $\mathbf{a} \geq 0$. Since $\mathbf{Q}$ and $\mathbf{S}$ have been defined as positive semidefinite and $\mathbf{R}$ has been defined as positive definite, $\mathbf{H} \geq 0$ and the cost function of the QP (37) is convex [12]. Since both constraint equations of the QP are affine, the QP is convex and $\mathbf{U}^{ol}$ is a global optimal solution of the QP.

E. Receding-Horizon Control

The state feedback spacing-control law used to perform the TM is computed using a receding-horizon approach. This approach can be described as follows. At each sampling time during the execution of the TM t, the ACC system measures the range, range rate, and ACC vehicle velocity and acceleration. Using these measurements, the SIVD is updated and, then, the error vector $\mathbf{e}(t)$ is computed. Using $\mathbf{e}(t)$ as the initial condition, the following QP is solved throughout the time horizon of the FTCOCP:

$$\min_{\mathbf{U}_t} \mathbf{U}_t^T\mathbf{H}\mathbf{U}_t + 2\mathbf{G}\big(\mathbf{e}(t)\big)\mathbf{U}_t \tag{40a}$$

subject to

$$\mathbf{L}_{\text{IN}}\mathbf{U}_t \leq \mathbf{M}_{\text{IN}}\big(\mathbf{e}(t)\big) \tag{40b}$$
$$\mathbf{L}_{EQ}\mathbf{U}_t = \mathbf{M}_{EQ}\big(\mathbf{e}(t)\big) \tag{40c}$$

where

$$\mathbf{U}_t = \begin{pmatrix} \mathbf{u}_t^* \\ \vdots \\ \mathbf{u}_{t+(N-1)}^* \end{pmatrix} \tag{41}$$

to obtain an optimal open-loop control sequence $\mathbf{U}_t^{ol}$. However, only the first acceleration command of this control sequence $\mathbf{u}_t^*$ is applied to the ACC vehicle.

If this process were to be repeated at each sampling time during the execution of the TM, then the acceleration command applied at each sampling time would be a function of the current measurements of range, range rate, and the ACC vehicle velocity and acceleration. Therefore, the spacing-control law applied to the ACC vehicle is a state feedback control sequence $\mathbf{U}^*$ where

$$\mathbf{U}^* = \begin{pmatrix} \mathbf{u}_0^* \\ \vdots \\ \mathbf{u}_{N_t-1}^* \end{pmatrix} \tag{42}$$

and where N_t is the time required to execute the TM.

In summary, the receding-horizon approach is used to determine the state feedback spacing-control laws for the TM problem using a series of FTCOCPs. It should be noted that the time horizon of the FTCOCP is shorter than the time horizon of the TM problem. Furthermore, it is assumed that the target vehicle has a constant acceleration during the online computation of the open-loop control sequence. Therefore, the MPC

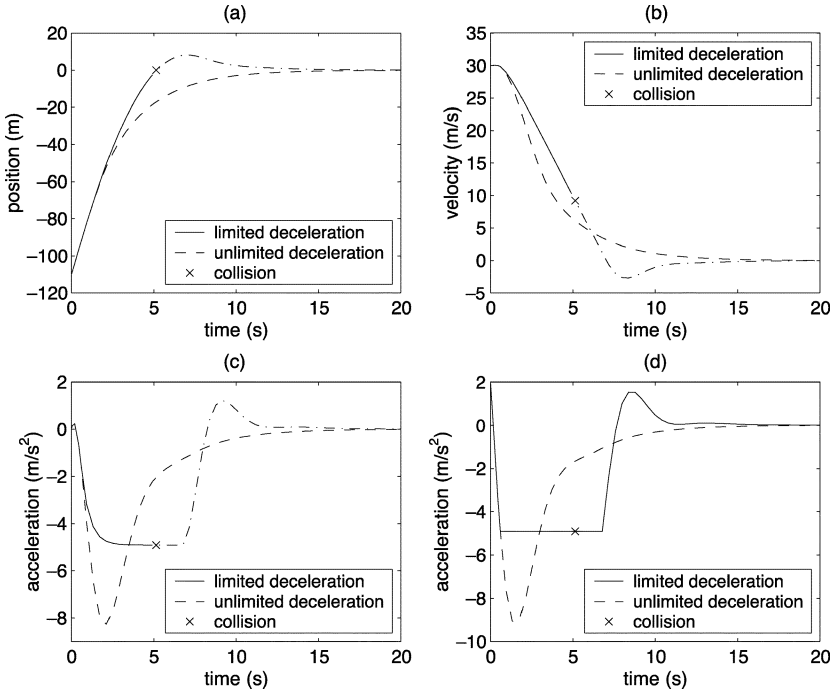

Fig. 5. ACC vehicle response, stalled target vehicle: CTG spacing-control law. (a) Relative ACC vehicle position, (b) absolute ACC vehicle velocity, (c) absolute ACC vehicle acceleration, and (d) commanded acceleration.

spacing-control law is designed to track the range and range rate.

IV. Simulation of the Spacing-Control Laws

The objective of the following simulations is to evaluate the performance of spacing-control laws used to execute a TM. The spacing-control laws will be computed using both the MPC algorithm and the CTG control algorithm. A baseline scenario requiring a TM will be established to evaluate and compare the two control algorithms. A spacing-control law will be considered successful if its application maneuvers the ACC vehicle to the SIVD with a zero-range rate while avoiding a collision with the target vehicle and satisfying the acceleration limits of the ACC vehicle. The computation of the spacing-control laws and the simulation of the ACC vehicle's response to these spacing-control laws were performed using Matlab.

A standard steady-state spacing policy adopted by the ACC system is the CTG spacing policy. The SIVD to be maintained by this spacing policy varies linearly with the velocity of the target vehicle such that the time headway between vehicles remains constant [4]. This SIVD can be defined as

$$\mathrm{SIVD} = \mathrm{h}v_0 \tag{43}$$

where h refers to the constant time headway between vehicles. It should be noted that the measurements of range rate and ACC vehicle velocity can be used to obtain the velocity of the target vehicle. The SIVD defined by this spacing policy will be used as the objective for all of the following simulations.

A. Baseline Scenario

The following scenario will be used to establish the baseline TM problem. In this scenario, the ACC vehicle is initially traveling at a speed of 30 m/s, with its speed-control mode enabled, when it encounters a stalled target vehicle at a range of 110 m. The TM required of the ACC vehicle is to decelerate to a complete stop behind the target vehicle. Since the velocity of the target vehicle is zero, the SIVD to be established by the ACC vehicle is 0 m. Throughout the entire TM, the TM frame has a velocity equal to zero and the target vehicle is located at the origin of the TM frame. Therefore, the ACC vehicle will have avoided a collision with the target vehicle if it does not cross the origin of the TM frame. The initial error vector can be defined as

$$\mathbf{e}(0) = \begin{pmatrix} -110\ \mathrm{m} \\ 30\ \mathrm{m/s} \\ 0 \end{pmatrix}. \tag{44}$$

This scenario is feasible because, given an initial range rate of 30 m/s, the ACC vehicle requires a minimum range of 106 m to decelerate to the velocity of the target vehicle (Fig. 4).

B. Simulation of the CTG Spacing-Control Law

The CTG control law can be defined as[5]

$$u_{\mathrm{CTG}}(t) = -\frac{1}{\mathrm{h}}\left(\dot{\mathrm{R}}(t) + \lambda\delta(t)\right) \tag{45}$$

where

$$\dot{\mathrm{R}}(t) = \dot{x}(t) - v_o(t) \tag{46}$$

$$\delta(t) = x(t) - x_o(t) + \mathrm{h}\dot{x}(t). \tag{47}$$

In (45), δ refers to the intervehicle spacing error. λ is a constant weighting factor between $\dot{\mathrm{R}}$ and δ.

The constants h and λ are selected to provide the vehicle with individual vehicle stability and string stability [3], [5]. A vehicle is considered to be individually stable if the spacing error between itself and the immediately preceding vehicle converges

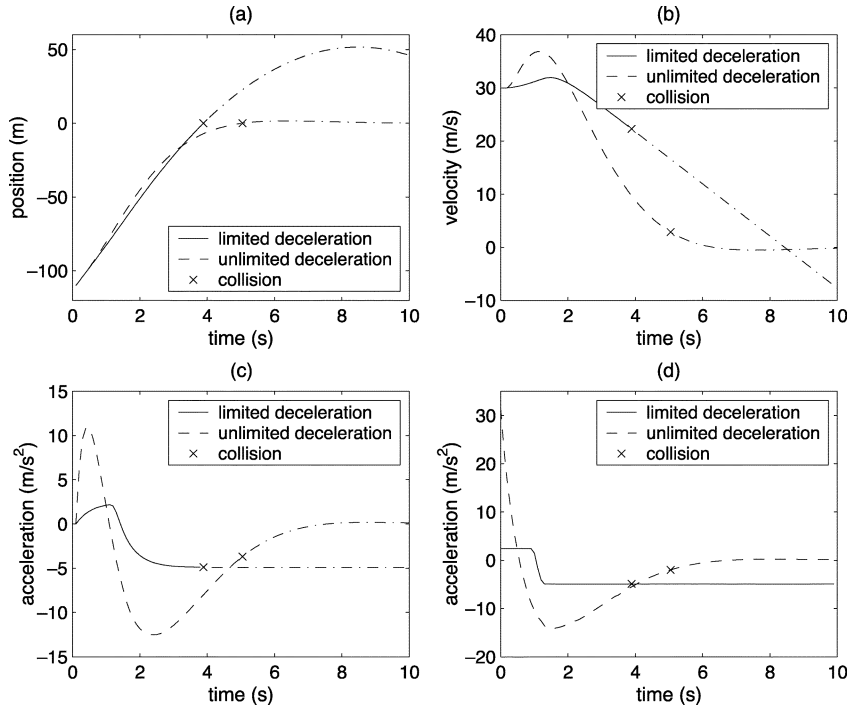

Fig. 6. ACC vehicle response, stalled target vehicle: unconstrained MPC spacing-control law. (a) Relative ACC vehicle position, (b) absolute ACC vehicle velocity, (c) absolute ACC vehicle acceleration, and (d) commanded acceleration.

to zero when the preceding vehicle is not accelerating. A vehicle will be individually stable if $\lambda > 0$. A vehicle formation is considered to be string stable if the intervehicle spacing errors do not amplify as the effects of a disturbance propagate to the tail of the formation. A vehicle formation will be string stable if $\mathrm{h} > 2\tau$. For the purposes of CTG control design and simulation, λ will be assumed to be equal to 0.4 and h will be selected as 1 s.

Fig. 5 shows the simulated response of the ACC vehicle to the CTG spacing-control laws computed for the TM of the baseline scenario. The dashed lines represent the spacing-control law and the subsequent response for the vehicle without deceleration limits. The solid lines represent the spacing-control law and the subsequent response for the vehicle with deceleration limits. In this case, if the command acceleration computed using (45) was less than the deceleration limit of the ACC vehicle, then the command acceleration was set equal to the deceleration limit. Fig. 5(a) shows that, in the case of unlimited deceleration, the ACC vehicle is able to successfully perform the TM. However, in the case of limited deceleration, the ACC vehicle is unable to successfully perform the TM and the ACC vehicle collides with the stalled target vehicle at a velocity of 8.94 m/s. The ACC vehicle velocity and acceleration at the time of the collision are indicated by an "x". The dashed/dotted lines show the response of the vehicle once it has crossed the SIVD and have been included for the ensuing analysis only.

Fig. 5(d) shows that the initial commands of the spacing-control law are to accelerate, thereby minimizing the intervehicle spacing error. These initial commands are then followed by commands to decelerate, thereby reducing the range rate. However, in this scenario, the ACC vehicle requires at least 106 m to decelerate to a complete stop. If the initial commands of the spacing-control law are to accelerate, then the deceleration limit prevents the ACC vehicle from applying the necessary braking to avoid a collision with the target vehicle. Therefore, the ACC vehicle must immediately begin to decelerate, rather than accelerate, to avoid a collision with the target vehicle.

The ACC vehicle is unable to perform the TM because the CTG algorithm does not include either the state constraints or the control constraints in its formulation. Therefore, the spacing-control law computed using the CTG control algorithm is concerned only with maneuvering the vehicle to the SIVD with a zero-range rate and is unable to account for the other requirements of the TM. The result is that the CTG spacing-control law maneuvers the vehicle across the SIVD and requires the vehicle to use a negative velocity to establish the SIVD.

C. Simulation of the MPC Spacing-Control Law

For the purposes of MPC control design and simulation, the sampling time T of the ACC vehicle model (8) was selected to be 0.1 s and the weighting matrices of the performance index (18) were selected as

$$\mathbf{Q} = \begin{pmatrix} 1 & 0 & 0 \\ 0 & 1 & 0 \\ 0 & 0 & 1 \end{pmatrix} \tag{48}$$

$$\mathbf{R} = (1) \tag{49}$$

$$\mathbf{S} = \begin{pmatrix} 1 & 0 & 0 \\ 0 & 1 & 0 \\ 0 & 0 & 1 \end{pmatrix}. \tag{50}$$

In the following figures, a collision between the ACC vehicle and the target vehicle is depicted in the same manner as in Fig. 5.

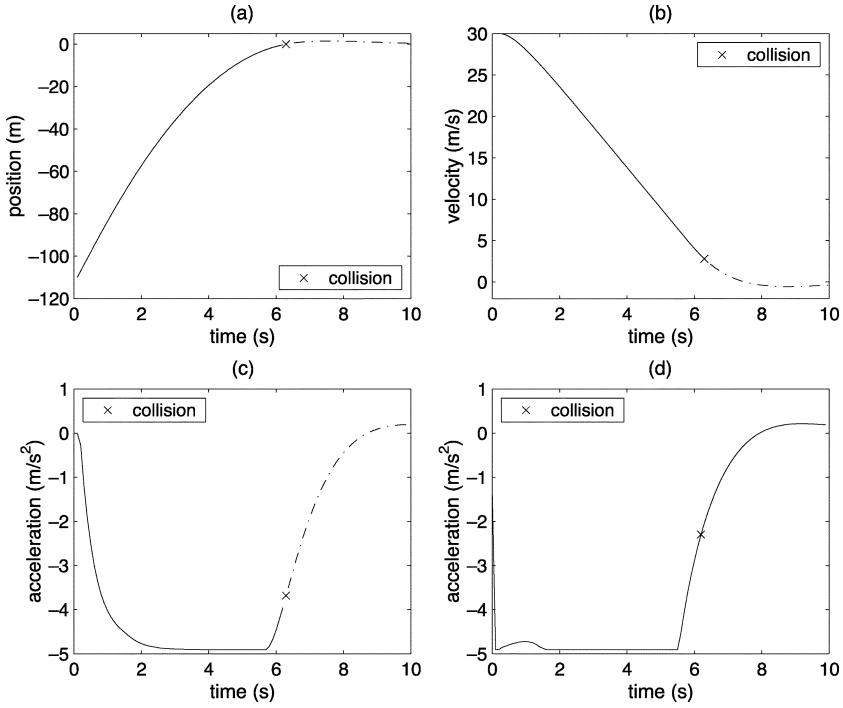

Fig. 7. ACC vehicle response, stalled target vehicle: partially constrained MPC spacing-control law. (a) Relative ACC vehicle position, (b) absolute ACC vehicle velocity, (c) absolute ACC vehicle acceleration, and (d) commanded acceleration.

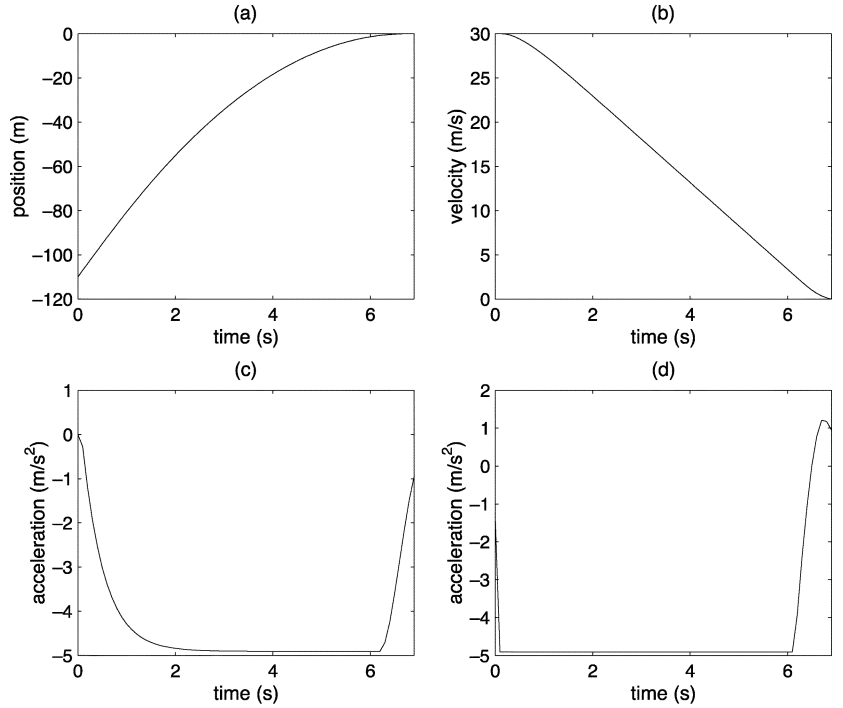

Fig. 8. ACC vehicle response, stalled target vehicle: MPC spacing-control law. (a) Relative ACC vehicle position, (b) absolute ACC vehicle velocity, (c) absolute ACC vehicle acceleration, and (d) commanded acceleration.

The ACC vehicle velocity and acceleration at the time of collision are indicated by an "x." The dashed/dotted lines show the response of the ACC vehicle once it has crossed the SIVD.

Figs. 6–8 show the simulated response of the ACC vehicle to the MPC spacing-control laws computed for the TM of the baseline scenario. For this scenario, the condition of a nonnegative ACC vehicle velocity was not included in the formulation of the FTCOCP. Since the target vehicle is stalled, the SIVD is zero and this vehicle is located at the origin of the TM frame. If the ACC vehicle were to cross the origin of the frame while performing the TM, then only a negative velocity would allow the ACC vehicle to establish the origin of the frame. Therefore, constraining the ACC vehicle velocity to be nonnegative would serve as an artificial collision avoidance condition.

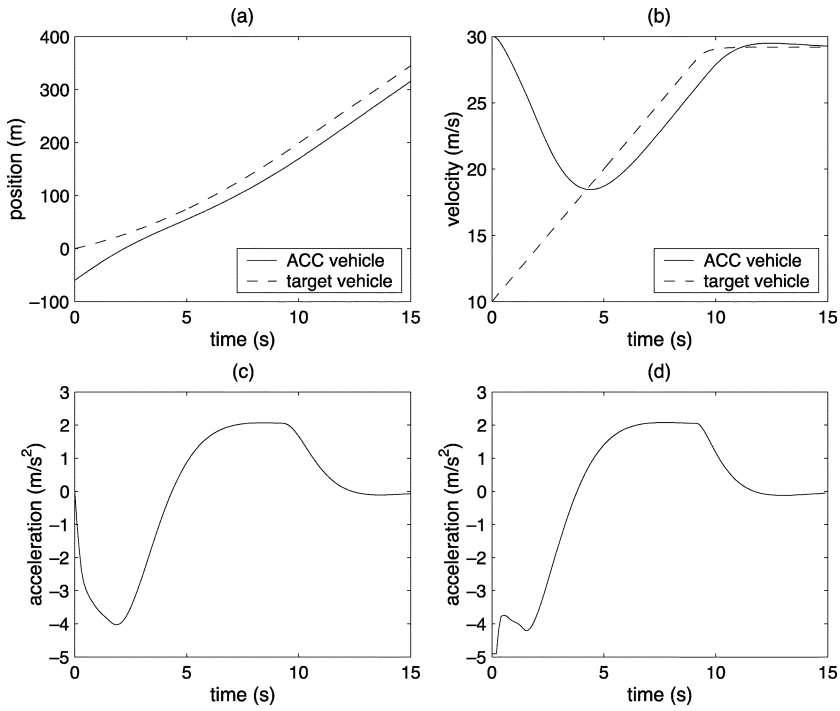

Fig. 9. ACC vehicle response, accelerating target vehicle: MPC spacing-control law. (a) Absolute vehicle positions, (b) absolute vehicle velocities, (c) absolute ACC vehicle acceleration, and (d) commanded acceleration.

Fig. 6 shows the response of the ACC vehicle to the MPC spacing-control law computed without including either collision avoidance or the acceleration limits of the ACC vehicle in the formulation of the FTCOCP. The QP formed from this FTCOCP includes equality constraints but does not include inequality constraints. These conditions are the same as those used to compute the CTG spacing-control law. The dashed lines represent the spacing-control law and the subsequent response for the vehicle without deceleration limits. The solid lines represent the spacing-control law and the subsequent response for a vehicle with deceleration limits. The deceleration limit was applied in the same manner as for the CTG spacing-control law. Fig. 6(a) shows that, in both cases, the ACC vehicle is unable to successfully perform the TM and the ACC vehicle collides with the stalled target vehicle at velocities of 2.82 and 22.82 m/s, respectively.

As in the case of the CTG spacing-control law, the initial commands of the MPC spacing-control law are to accelerate followed by commands to decelerate. Since collision avoidance and the acceleration limits have not been incorporated into the FTCOCP, the MPC control law is concerned only with maneuvering the ACC vehicle to the final state constraint. In this case, the spacing-control law is governed only by the weighting matrices of the performance index. The result is that this MPC spacing-control law maneuvers the vehicle across the SIVD and requires the vehicle to use a negative velocity to establish the SIVD.

Fig. 7 shows the response of the ACC vehicle to the MPC spacing-control law computed without collision avoidance, but with the acceleration limits of the ACC vehicle included in the formulation of the FTCOCP. The QP formed from this FTCOCP includes the equality constraints and the inequality constraints derived from the acceleration limits. Fig. 7(a) shows that the ACC vehicle is unable to successfully perform the TM and that the ACC vehicle collides with the stalled target vehicle at a velocity of 2.80 m/s. This MPC spacing-control law maneuvers the vehicle across the SIVD and requires the vehicle to use a negative velocity to establish the SIVD.

Fig. 8 shows the response of the ACC vehicle to the MPC spacing-control law with both collision avoidance and the acceleration limits of the ACC vehicle included in the formulation of the FTCOCP. The QP formed from this FTCOCP includes the complete set of equality and inequality constraints as described in Section III. Fig. 8(a) shows that the ACC vehicle is able to successfully perform the TM, as the ACC vehicle establishes the SIVD with a zero-range rate. In this case, the simulation was stopped when the ACC vehicle decelerated to a complete stop.

Figs. 7(d) and 8(d) show that when the acceleration limits are included in the formulation of the FTCOCP, the initial commands of the spacing-control law are to decelerate. The difference between the two spacing-control laws is the length of the braking time commanded by the spacing-control law. Only when collision avoidance is specifically included in the FTCOCP does the spacing-control law ensure that the ACC vehicle establishes a zero-range rate before the vehicle crosses the origin of the TM frame. Therefore, both collision avoidance and the acceleration limits of the ACC vehicle must be specifically incorporated into the formulation of the FTCOCP to ensure that the spacing-control law is able to successfully maneuver the ACC vehicle to the SIVD.

To further evaluate the performance of the MPC control algorithm, a second scenario was considered in which the ACC vehicle encounters an accelerating target vehicle. In this scenario, the ACC vehicle is initially traveling at a speed of 30 m/s with its

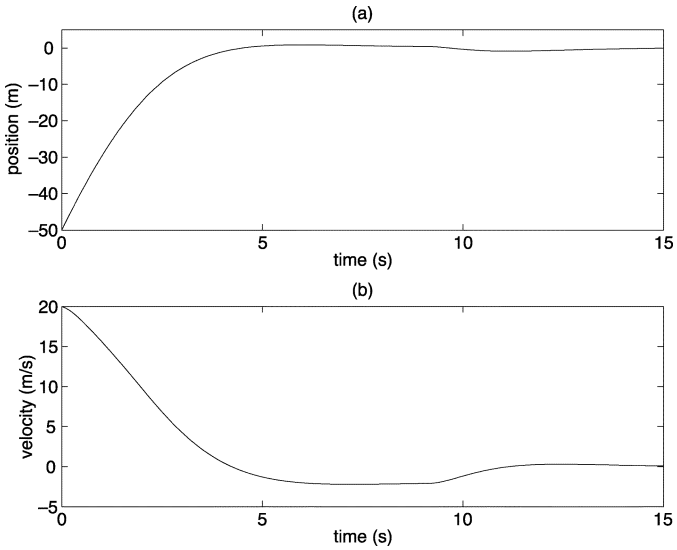

Fig. 10. ACC vehicle response, accelerating target vehicle: MPC spacing-control law. (a) Relative ACC vehicle position and (b) range rate.

speed-control mode enabled when it encounters an accelerating target vehicle at a range of 60 m and a range rate of 20 m/s. The target vehicle accelerates at 2 m/s^2 to establish and then maintain a speed of 29 m/s. During this maneuver, the SIVD continuously changes from 10 m, initially, to 29 m, finally. The TM required of the ACC vehicle is to establish the SIVD with a zero-range rate while the target vehicle performs its entire maneuver. The initial error vector can be defined as

$$\mathbf{e}(0) = \begin{pmatrix} -50\ \mathrm{m} \\ 20\ \mathrm{m/s} \\ 0 \end{pmatrix}. \tag{51}$$

Figs. 9 and 10 show the simulated response of the ACC vehicle to the MPC spacing-control laws computed for the TM of the second scenario. These spacing-control laws were computed using the complete set of equality and inequality constraints as described in Section III. Fig. 9 shows the absolute position, velocity, and acceleration of the ACC vehicle. Fig. 10 shows the relative position and velocity of the ACC vehicle in the TM frame.

Fig. 9(d) shows that the MPC spacing-control law initially commands a deceleration to reduce the range rate as the ACC vehicle approaches the SIVD. However, as the ACC vehicle approaches the SIVD, the target vehicle is still accelerating and, thus, the SIVD is increasing. The spacing-control law responds to the target vehicle's maneuver by commanding the ACC vehicle to accelerate to track the SIVD. However, as the ACC vehicle increases its acceleration to 2 m/s^2, Fig. 10(d) shows that the ACC vehicle maintains a range rate of -2.2 m/s. The spacing-control law maintains a negative range rate to ensure the range increases as the ACC vehicle tracks the increasing SIVD. Once the target vehicle establishes and maintains a speed of 29 m/s, the spacing-control law reduces the command acceleration so that the ACC vehicle establishes the SIVD with a zero-range rate.

V. Conclusion

In this paper, MPC was used to compute the spacing-control laws for TMs of ACC vehicles. It was shown how to obtain the MPC spacing-control laws by formulating the objective and requirements of the TM problem as a constrained OCP and by solving this constrained OCP by using a receding-horizon approach. A baseline scenario requiring a TM was used to evaluate and compare the simulated response of the ACC vehicle to the spacing-control laws computed using the MPC algorithm and the CTG control algorithm. These simulations showed that collision avoidance and the acceleration limits of the ACC vehicle must be explicitly incorporated into the formulation of the control algorithm to successfully perform the TM for all feasible scenarios that require a TM.

These MPC spacing-control laws have been designed to perform longitudinal vehicle control only. Infeasible encounter scenarios will result in a collision between the ACC vehicle and the target vehicle. These scenarios require driver interaction to avoid a collision and require further study involving driver interaction with the ACC system.

The following aspects of the MPC spacing-control law are also currently being studied. First, the effect of sensor noise on the computation of the SIVD and the MPC spacing-control laws is being investigated. For example, the definition of the required range for feasible encounter scenarios must be increased to reflect the uncertainty of the sensor measurements. Second, the online computation of the MPC spacing-control laws and the ability of these spacing-control laws to provide string stability are being investigated as well.

References

[1] K. Santhanakrishnan and R. Rajamani, "On spacing policies for highway vehicle automation," *IEEE Trans. Intell. Transport. Syst.*, vol. 4, pp. 198–204, Dec. 2003.

[2] P. Fancher and Z. Bareket, "Evaluating headway control using range versus range-rate relationships," *Veh. Syst. Dyn.*, vol. 23, pp. 575–596, 1994.

[3] D. Swaroop and J. K. Hedrick, "String stability of interconnected systems," *IEEE Trans. Automat. Contr.*, vol. 41, pp. 349–357, Mar. 1996.

[4] R. J. Caudill and W. L. Garrard, "Vehicle-follower longitudinal control for automated transit vehicles," *J. Dyn. Syst., Meas., Control*, vol. 99, pp. 241–248, 1977.

[5] D. Swaroop and J. K. Hedrick, "Constant spacing strategies for platooning in automated highway systems," *J. Dyn. Syst., Meas., Control*, vol. 121, pp. 462–470, 1999.

[6] V. K. Narendran, J. K. Hedrick, and K. S. Chang, "Merge control of vehicles in an automated highway system," in *Proc. 3rd ASME Symp. Transportation Systems*, vol. DSC-44, 1992, pp. 269–279.

[7] J. Frankel, L. Alvarez, R. Horowitz, and P. Li, "Safety oriented maneuvers for IVHS," *Veh. Syst. Dyn.*, vol. 26, pp. 271–299, 1996.

[8] P. Li, L. Alvarez, and R. Horowitz, "AHS safe control laws for platoon leaders," *IEEE Trans. Control Syst. Technol.*, vol. 5, pp. 614–628, Nov. 1997.

[9] T. R. Connolly and J. K. Hedrick, "Longitudinal transition maneuvers in an automated highway system," *J. Dyn. Syst., Meas., Control*, vol. 121, pp. 471–478, 1999.

[10] D. Q. Mayne *et al.*, "Constrained model predictive control: stability and optimality," *Automatica*, vol. 36, pp. 789–814, 2000.

[11] G. C. Goodwin, S. F. Graebe, and M. E. Salgado, *Control System Design*. Englewood Cliffs, NJ: Prentice-Hall, 2001, pp. 739–765.

[12] F. Borrelli, *Constrained Optimal Control of Linear and Hybrid Systems*, ser. Lecture Notes Control Inform. Sci. 290. New York: Springer-Verlag, 2003, pp. 51–101.

[13] D. G. Hull, "Conversion of optimal control problems into parameter optimization problems," *J. Guid., Control, Dyn.*, vol. 20, no. 1, pp. 57–60, 1997.

[14] C. T. Chen, *Linear System Theory and Design*, 3rd ed. New York: Oxford Univ. Press, 1999, pp. 86–120.
[15] A. E. Bryson, *Dynamic Optimization*. Menlo Park, CA: Addison-Wesley, 1999, pp. 201–260.
[16] S. Boyd and L. Vandenberghe, *Convex Optimization*. New York: Cambridge Univ. Press, 2004.

Vibhor L. Bageshwar received the B.A.Sc. and M.A.Sc. degrees in aerospace engineering from the University of Toronto, Toronto, ON, Canada, and the M.S. degree in aerospace engineering from the University of Minnesota, Minneapolis, where he is currently working toward the Ph.D. degree.

His current research interests include the application of estimation and control theory to both aerospace and ground vehicles.

William L. Garrard received the B.S. degree in mechanical engineering and the Ph.D. degree in engineering mechanics from the University of Texas, Austin.

He joined the faculty of the University of Minnesota, Minneapolis, in December 1967, where he currently is a Professor and Head of the Department of Aerospace Engineering and Mechanics. During 1995, he was a Visiting Scientist with CERT/ONERA in Toulouse, France. He has published over 100 technical papers and has received external research funding from the National Aeronautics and Space Administration (NASA), National Science Foundation (NSF), U.S. Department of Transportation, the Air Force Office of Scientific Research, Army Research Office, Sandia Laboratories, and private industry. His research areas are in the application of advanced control theory to aerospace vehicles and parachute systems.

Dr. Garrard received the Educational Award for Excellence from the U.S. Army Soldier System Command for his work in parachute systems in 1996. He is an Associate Fellow of the American Institute Aeronautics and Astronautics (AIAA). In 2003, he was awarded a Certificate of Appreciation by the AIAA in recognition for his many years of organizing, coordinating, and conducting the H. G. Heinrich Parachute Systems Short Course and for the large number of parachute engineers it has produced. He is Director of the NASA-funded Minnesota Space Grant Consortium and currently is one of the AIAA Commissioners on the Engineering Accreditation Commission of Accreditation Board for Engineering and Technology (ABET).

Rajesh Rajamani (M'94) received the B.Tech. degree from the Indian Institute of Technology, Madras, in 1989 and the M.S. and Ph.D. degrees from the University of California, Berkeley, in 1991 and 1993, respectively.

After receiving the Ph.D. degree, he spent five years as a Research Engineer, first at the United Technologies Research Center (UTRC), CT, and then at California PATH, Berkeley. Currently, he is an Associate Professor in the Department of Mechanical Engineering, University of Minnesota, Minneapolis. He has authored over 60 refereed publications and has received two patents. His active research interests include intelligent transportation systems, active noise control, MEMS sensor design, fault diagnostics, and control design and state estimation for nonlinear systems.

He has won several awards, including the CAREER Award from the National Science Foundation, the 2001 Outstanding Paper Award from the IEEE TRANSACTIONS ON CONTROL SYSTEMS TECHNOLOGY, the Distinguished Service Team Award from the University of California, Berkeley, and the Outstanding Achievement of the Year Award from the United Technologies Research Center.